Satellite estimation of spectral surface UV irradiance
2: Effect of horizontally homogeneous clouds

N.Krotkov[1], J.R. Herman[2], P.K. Bhartia[2], Z. Ahmad[3], V. Fioletov[4]

November 2, 1998
Submitted to ECUV Conference Special Issue

---

[1] Raytheon ITSS 4400 Forbes Blvd. Lanham, MD. 20706

[2] Goddard Space Flight Center, Code 916, Greenbelt, MD 20771

[3] Science and Data Systems, Silver Spring, MD.

[4] Atmospheric Environmental Service, Toronto, Canada

Abstract The local variability of UV irradiance at the Earth's surface is mostly caused by clouds in addition to the seasonal variability. Parametric representations of radiative transfer RT calculations are presented for the convenient solution of the transmission T of ultraviolet radiation through plane parallel clouds over a surface with reflectivity R_S . The calculations are intended for use with the Total Ozone Mapping Spectrometer (TOMS) measured radiances to obtain the calculated Lambert equivalent scene reflectivity R for scenes with and without clouds. The purpose is to extend the theoretical analysis of the estimation of UV irradiance from satellite data for a cloudy atmosphere. Results are presented for a range of cloud optical depths and solar zenith angles for the cases of clouds over a low reflectivity surface $R_S<0.1$, over a snow or ice surface $R_S>0.3$, and for transmission through a non-conservative scattering cloud with single scattering albedo $\omega_o = 0.999$. The key finding for conservative scattering is that the cloud-transmission function C_T , the ratio of cloudy- to clear-sky transmission, is roughly $C_T = 1 - R_C$ with an error of less than 20% for nearly overhead sun and snow-free surfaces. For TOMS estimates of UV irradiance in the presence of both snow and clouds, independent information about snow albedo is needed for conservative cloud scattering. For non-conservative scattering with $R_S>0.5$ (snow) the satellite measured scene reflectance cannot be used to estimate surface irradiance. The cloud transmission function has been applied to the calculation of UV irradiance at the Earth's surface and compared with ground-based measurements [*Herman et al.*, 1998].

1. Introduction

Changes in cloudiness produce the strongest source of the local variability in the surface UV irradiance [*Madronich 1993*]. Since any current satellite view is an average over an extended area, the satellite method of mapping surface (UV or PAR) irradiance has to address cloud variability within its field of view FOV. Frederick and Lubin [1988] suggested the use of average UV reflectance within the FOV (170km X 170km) of the Solar Backscatter Ultraviolet (SBUV) instrument to derive UV transmittance through clouds.

The availability of the daily global imagery from the Advanced Very High Resolution Radiometer (AVHRR) instruments aboard the NOAA polar orbiting satellites makes it possible to estimate the cloud transmittance with a higher spatial resolution (~ 2km for local area coverage data and 4km for the global area coverage) than for TOMS observations. The sucessful applications of the AVHRR techniques to UV-irradiance mapping have been demonstrated so far only for local geographical areas: Germany [*Meerkoetter et al 1997*], Antarctic Peninsula [*Lubin et al., 1994*], and Moscow region, Russia [*Rublev et al., 1997*]. Although global (GAC) AVHRR data are available (at least for last several years), the technical difficulties (different satellites, calibration issues, large volumes of data, data gaps) prevent using AVHRR data for surface UV irradiance maping on the global scale.

Another suggested approach is to combine the TOMS ozone data with shortwave cloud reflectance measurements from the NASA Earth Radiation Budget Experiment (ERBE) [*Lubin and Jensen 1995; Lubin et al., 1998*]. The ERBE data set is available only since 1985 *[Lubin 1998*]. Also, the transmittance of the cloudy atmosphere is spectrally dependent in the near UV and visible spectral regions [*Nack and Green, 1974; Seckmeyer et al.*,1997; *Krotkov et al.*,1997;

Frederick and Erlick, 1997]. Therefore, the extrapolation of the spectrally integrated shortwave ERBE measurements into the UV spectral region is not straightforward and requires further justification.

Surface UV irradiance data derived from TOMS ozone and UV-reflectivity data are based on a single well-calibrated instrument [*Eck et al., 1987; Eck et al. 1995*]. Using total ozone and 380nm reflectivity measurements from the TOMS instrument aboard the Nimbus-7 satellite, Herman et al. [1996] have estimated the zonal average trends in surface UV flux between January 1979 and December 1992, while neglecting absorbing aerosols. Because of long time record (since 1978) and contiguous global spatial coverage, TOMS data are vital not only for estimating zonal average trends in surface UV flux [*Madronich 1992; Herman et al. 1996*], but also in studying geographical differences in surface UV climatology, including effects of clouds and aerosols [*Herman et al., 1998*].

Krotkov et al [1998] examined a UV-mapping algorithm that included aerosol attenuation for cloud- and snow- free conditions, and compared calculated UV irradiances with ground-based data. In the absence of clouds and absorbing aerosols (or for known aerosol amounts), it was demonstrated that satellite measurements of extraterrestrial solar flux, total ozone and UV reflectivity (at 0.36 or 0.38μm) can be used in conjunction with a radiative transfer model to provide estimates of surface spectral UV irradiance to accuracies comparable to that of well maintained ground-based instruments (e.g., Toronto Brewer).

The purpose of the present paper is to extend the theoretical basis of the clear-sky analysis for estimation of surface-UV irradiance from TOMS measured radiances to the case for a cloudy aerosol-free atmosphere with ozone absorption. We also assume a spectrally independent (grey) cloud optical thickness for simulation of the backscattered radiance at the top of the atmosphere and the UV irradiance at the Earth's surface. An issue of concern is the use of satellite measured radiances to estimate an approximation to the hemispherical cloud albedo in the 100x100 km^2 field of view (FOV). The approximation is based on the assumption that the mixture of cloud-surfaces in the FOV can be represented by a Lambertian equivalent reflectivity (LER) or a plane parallel cloud. The case of a mixture of clear and cloudy scenes within the satellite FOV will be discussed in a future paper.

In section 2 we discuss the relationship between hemispherical albedo of the cloud layer and spectral transmittance of a cloudy atmosphere over snow-free surfaces (low reflectivity). Section 3 uses these results to discuss satellite estimation of the cloud albedo for snow-free conditions. The sensitivity to the presence of snow is discussed in section 4. Section 5 discusses the combining effects of clouds and absorbing (soot) aerosols on the UV atmospheric transmittance.

2. Relationship between cloud albedo and cloud factor

The effect of clouds on global (direct plus diffuse) UV irradiance at the Earth's surface can be described by a relative atmospheric transmittance function, which will be referred to as

the measured Cloud Transmission function C_{TG} from ground-based measurements (see Equation 1).

$$F_{cloud}(\theta_o, O_3, \lambda) = F_{clear}(\theta_o, O_3, \lambda)\, C_{TG}(\theta_o, O_3, \lambda) \quad (1)$$

F_{cloud}, is the measured spectral surface irradiance for cloudy conditions,
F_{clear} is the estimated clear sky irradiance (the same atmosphere but with the clouds removed).
λ is the wavelength.
θ_o is the solar zenith angle.

The calculation of F_{clear} from the satellite measurements of the extraterrestrial solar irradiance, total column ozone O_3 and surface reflectivity R_S were discussed in *Krotkov et al.* [1998]. Here we focus on the theoretical estimation of the C_T using the TOMS satellite reflectivity-channel wavelengths, 360 or 380 nm. For this analysis we define C_T as the ratio of the calculated atmospheric transmittances using aerosol-free atmospheric models:

$$C_T(\lambda, \theta_o, O_3) = T_{cloud} / T_{clear} \quad (2)$$

2.1 Cloud Without an Atmosphere

Some of the characteristics of the cloud transmission function can be investigated for the simple case of a cloud over a surface with reflectivity R_S. Assuming a horizontally-homogeneous plane-parallel conservative-scattering cloud, and neglecting atmospheric scattering and absorption (T_{clear}=1), C_T can be formally expressed as a solution of the Stoke's problem [*Chandrasekhar, 1960*]:

$$C_T = [1 - R_C] / [1 - R_S R^{Dif}_C] \quad (3)$$

where R_C is the hemispherical albedo of the cloud layer illuminated by direct solar beam for zero surface reflectivity (R_S=0) and R^{Dif}_C is the albedo of the same cloud illuminated by diffuse source (see Figure 1). In the near-UV spectral region R_S is low (2 to 8%) for snow- and ice-free surfaces [*Eck et al.* 1987; *McKenzie et al.*, 1996; *Herman and Celarier* 1997]. Neglecting the surface reflection (the general case of arbitrary R_S will be discussed further in section 4):

$$C_T(\theta_0, \tau_C, \chi) = [1 - R_C] \quad (4)$$

For conservative scattering R_C is a unique solution of the multiple scattering radiative transfer problem for a given cloud phase function, γ_C, optical thickness, τ_C, and solar zenith angle, θ. The phase function γ_C is determined by the cloud-droplet size distribution. For this analysis we use the C1-cloud model [*Deirmendjian* 1969]. Figure 1 shows the dependence of R_C on τ_C and μ_O=cos θ_0 calculated using both numeric (DISORT [*Stamnes et al.*,1988]) and approximate (two-stream) [*Coakley and Chylek*, 1975] solutions:

$$R_C = \tau_C^* / (\tau_C^* + 2\mu_0) \tag{5}$$

where $\tau_C^* = (1-g)\tau_C$ is the cloud effective optical thickness, g is the asymmetry factor (mean cosine of γ_C ; g= 0.848 for C1 cloud), and $\mu_0 = \cos\theta_0$. The accuracy of different two-stream approximations is discussed in many papers [*King* 1985; *Lenoble* 1993; *Liou* 1993]. Here we use Equation 5 and the radiative transfer calculation (DISORT) to illustrate some general properties of R_C: As shown in Figure 1,

- For a given μ_0, R_C is a non-linear monotonically increasing function of τ_C^*
- For a fixed τ_C , R_C is minimal for overhead sun and increases with increase in θ_0.

This implies that a cloud layer can reflect a greater percentage of the incident radiation when illuminated by diffuse source than it does for nearly normally incident solar irradiance. The ratio of the upward irradiance to the downward irradiance for diffuse illumination is:

$$R_C^{Diffuse} = 2\int_0^1 R_C(\mu_o)\,\mu_o\,d\mu_o \tag{6a}$$

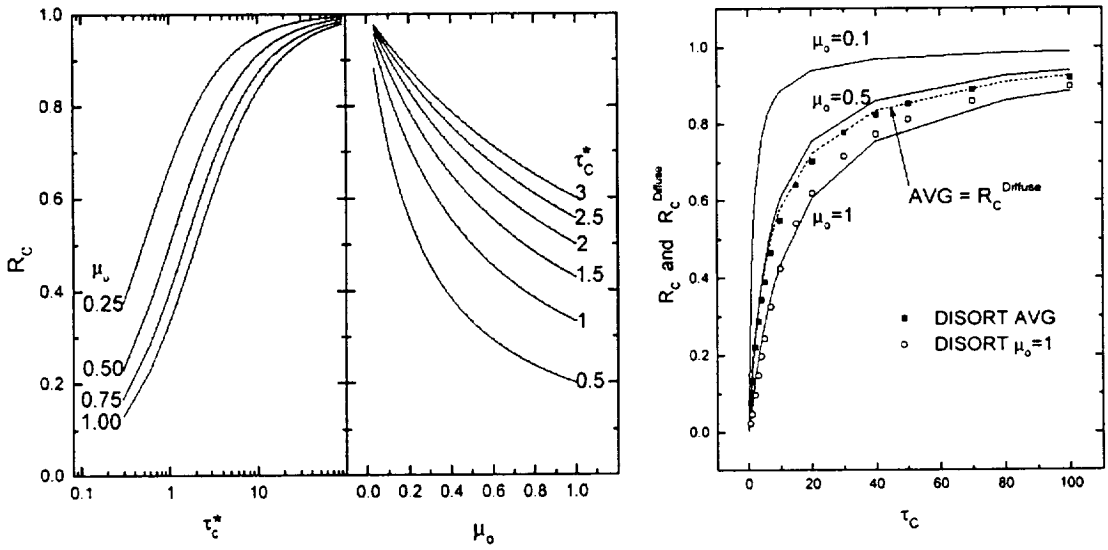

Figure 1 Cloud albedos R_C and R_C^{Dif} as a function of τ_C or τ_C^* and $\mu_0 = \cos(\theta_0)$. The discrete points are from the DISORT calculation and the continuous lines are from the Equations 5 and 6.

$$R_C^{Dif} = \tau_C^* \left[1 - 0.5\tau_C^* \ln(1 + \frac{2}{\tau_C^*}) \right] \tag{6b}$$

One important consequence of $R_C^{Dif} > R_C(\mu_o \approx 1)$ is the theoretical possibility of apparent enhanced cloud transmittance ($C_T>1$) over bright snow surface (discussed later in section 4), since the top of the cloud is illuminated by the direct sun while the bottom of the cloud is illuminated by diffuse radiation reflected from the snow [*Shettle and Weinman, 1970*].

- If τ_C is parameterized in terms of the column liquid water content, W (usually in units of grams per m^2), and the effective radius of the droplet size distribution, r_{eff}, then $\tau_C \sim 1.5W/r_{eff}$ [*Stephens*, 1978]. For a given water content and solar zenith angle (W=const, μ_0 =const), increasing the effective radius of cloud droplets results in increasing cloud transmission C_T (see Figure 1 and Equation 5).

Even though we neglect spectral dependence of τ_C^*, the strong spectral dependence of Rayleigh scattering ($\sim\lambda^{-4}$) and ozone absorption in the UV-B spectral region (290 to 320 nm) causes the combined relative transmittance C_T of the cloud plus atmosphere (Equation 2) to be spectrally dependent and usually larger than 1- R_C (from Equation 4). In the next section we consider these atmospheric effects.

2.1 Atmospheric Effects

To study the sensitivity of C_T to atmospheric parameters and the relationship with cloud co-albedo (1-R_C), we consider a model that includes a homogeneous water-cloud layer of optical depth τ_C embedded in a scattering molecular atmosphere with ozone absorption.

Using calculated values of T_{clear} and T_{cloud}, C_T is calculated from Equation (2) in the UV spectral region (290-400nm) for a wide range of input atmospheric parameters and solar zenith angles θ_0=0-70°. For a cloud- and aerosol-free atmosphere with a Lambertian reflecting surface, the atmospheric transmittance T_{clear} is calculated for each wavelength from

$$T_{clear} = (T_{dir} + T_{diff}) \; / \; (1-R_S \, S_b), \tag{7}$$

where T_{dir} and T_{diff} are the direct and diffuse irradiance at the ground for unit solar flux and zero surface reflectivity [*Chandresekhar, 1960*]. The factor $(1-R_S \, S_b)^{-1}$ accounts for the effect of surface reflectivity, where S_b is the fraction of reflected radiation backscattered to the surface by the cloud-free atmosphere and R_S is the surface reflectivity (albedo). We calculate the various terms in Equation 7 for a Rayleigh atmosphere with standard ozone profiles [*McPeters et al.*, 1996; *Wellemeyer et al.*, 1997] using numerical solutions of the DISORT radiative transfer equation for large optical thicknesses where polarization can be neglected, and for modified versions of the Gauss-Seidel code [*Herman and Browing* 1965; *Ahmad and Frazer, 1982*] for smaller optical depths where polarization can have a noticeable effect on radiances at the ground and the top of the atmosphere.

The high-spectral resolution (0.05nm) temperature-dependent ozone-absorption coefficients are based on the laboratory measurements of *Bass and Paur* [1985] and the Rayleigh scattering coefficients from *Bates* [1984]. We use the same atmospheric model with an

embedded horizontally homogeneous water cloud to calculate T_{cloud}. The cloud parameters are the cloud base and top altitudes, cloud optical thickness τ_C, and the cloud phase function γ_C. τ_C is assumed spectrally independent and γ corresponds to C1-cloud model [*Deirmendjian* 1969]. The effective phase function is determined as a mixture of the cloud and Rayleigh phase functions for each computational layer $\Delta\tau_C$, and is wavelength dependent through the scattering mixing ratio $(\Delta\tau_C / \Delta\tau_{rayleigh}(\lambda))$.

2.2.1 C_T Spectral Dependence

Figure 2 shows the calculated spectral dependence of atmospheric transmittance for clear (T_{clear}) and cloudy (T_{cloud}) conditions as well as $C_T(\lambda)=T_{cloud}/T_{clear}$.

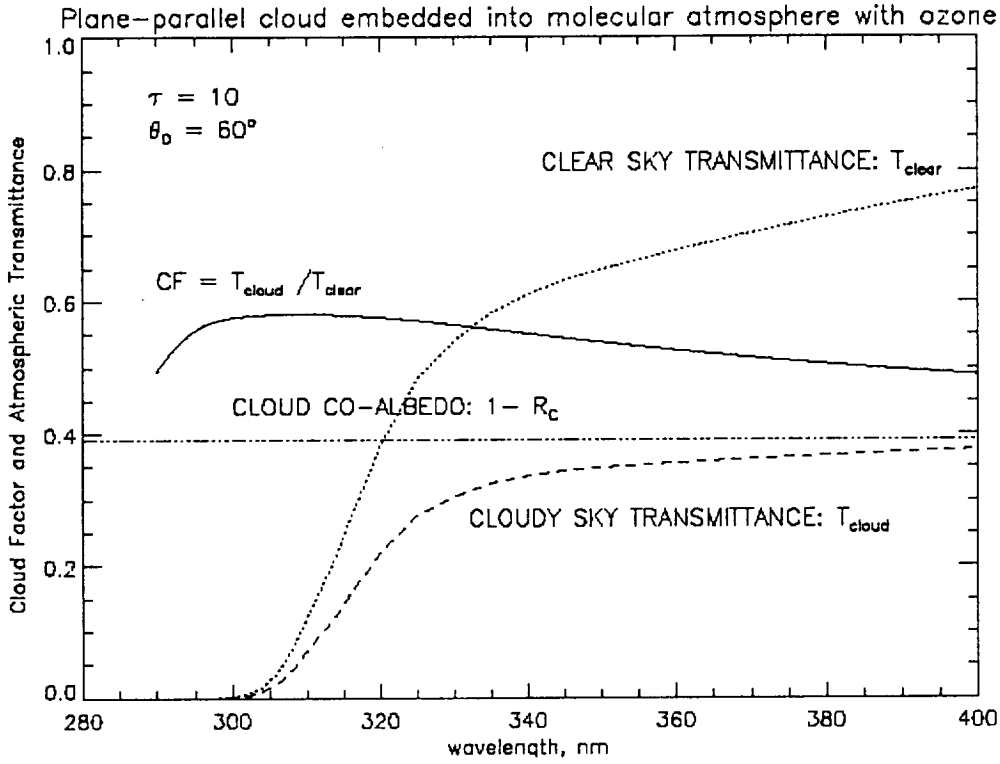

Figure 2 Spectral dependence of C_T, T_{clear}, and T_{cloud} (290nm-400nm) for τ_C=10.

Both T_{cloud} and T_{clear} decrease at shorter UV-A wavelengths (320-400nm) due to increasing molecular scattering ($\tau_R(\lambda) \sim \lambda^{-4}$). Ozone absorption is weak in the UVA spectral region, but increases exponentially at shorter UVB wavelengths (λ<320nm). Because of stratospheric ozone absorption (maximum ozone concentration at 25 km) the atmospheric transmittance drops several orders of magnitude at shorter UVB wavelengths. The effect of stratospheric ozone absorption on C_T is canceled by calculating the ratio T_{cloud}/T_{clear} for the same ozone amount. As a result, $C_T(\lambda)=T_{cloud}/T_{clear}$ is a weak function of wavelength in the UVA

(320nm-400nm) spectral region, and only shows ozone effects from multiple scattering within the cloud for the shortest wavelengths (maximum ozone absorption). Using C_T to estimate cloud transmittance in the UV is useful because of the independence of C_T from stratospheric ozone absorption, with only a weak dependence on tropospheric absorption at the shortest wavelengths of interest (λ <300 nm), except for clouds with greater altitude thickness (e.g., thunderstorms, *Mayer et al., 1998*)

The residual spectral dependence of C_T(~20%) (see Figure 2) is due to second order effects, which remain after the cancellation of the first order effects (i.e. stratospheric ozone absorption). Multiple reflections between the cloud layer and Rayleigh atmosphere tend to increase C_T much like reflection from the ground (Equation 3). On the other hand, enhancement in tropospheric ozone absorption in the presence of clouds tends to decrease C_T. As a result, the spectral dependence of $C_T(\lambda)$ has a broad maximum at 300-330nm, with a decrease longward of the maximum (due to decreasing of $\tau_R(\lambda) \sim \lambda^{-4}$), and a sharp decrease shortward (due to the spectral enhancement of absorption by tropospheric ozone).

To illustrate the behavior of $C_T(\lambda)$ it is convenient to parameterize the spectral dependence by normalizing at a specific wavelength λ_0:

$$C_T(\lambda) = S_C(\lambda, \theta_o, \tau_C)\, C_T(\lambda_0) \tag{8}$$

Where $S_C(\lambda) = C_T(\lambda)/C_T(\lambda_0)$, and λ_0 is any UVA wavelength, where ozone absorption is negligible. Figure 3 shows the wavelength dependence of $S_C(\lambda, \theta_o, \tau_C)$ for $\theta_o = 0°$ and 70° and τ_C=1, 3, 5, and 10. This shows that the wavelength dependence increases strongly with increasing θ_o, and with increasing τ_C. Thus, the atmosphere/cloud system, with a spectrally independent τ_C becomes relatively more transparent in the UVB than in the UVA (320-400nm) and visible spectral regions [*Nack and Green, 1974; Seckmeyer et al.*,1997; *Krotkov et al.*, 1997; *Frederick and Erlick*, 1997].

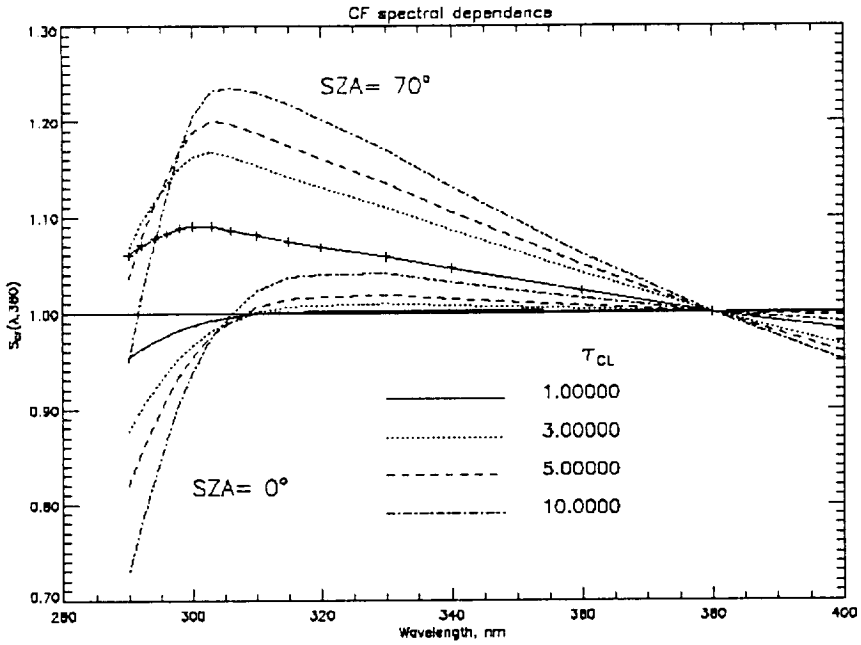

Figure 3 The spectral dependence factor $S_C(\lambda=380, \theta_o, \tau_C)$ for θ_o = 0° and 70°.

2.2.2 C_T Dependence on Cloud Optical Depth

For overhead sun and a dark surface below the cloud, Figure 4 shows that the dependence of C_T on τ_C is roughly the same as the dependence of $(1-R_C)$ on τ_C (see Equation 5). This is consistent with the assumed cloud transmittance used in previous studies [*Eck et al.*, 1995; *Herman et al.*, 1996]. At weakly ozone absorbing wavelengths (315-400nm) C_T is larger than $(1-R_C)$ due to the Rayleigh backscatter effect from the atmosphere above the cloud. The increase is 10 to 12% at τ_C=20. However, at strongly ozone absorbing wavelengths (<300nm), C_T becomes smaller than $(1-R_C)$, due to enhancement in tropospheric ozone absorption compared to longer wavelengths. At 294 nm and τ_C=20 the decrease is about 13%. In the limiting cases of very small (τ_C<1) or extremely high (τ_C>100) cloud optical depths, C_T approaches $(1-R_C)$ for wavelengths where there is little or no ozone absorption. When there is ozone absorption (see Figure 4 for 294 nm) and the cloud optical depth τ_C>1, tropospheric ozone absorption is enhanced within the cloud leading to deviations from $1-R_C$. The optical depth at which C_T deviates from $1-R_C$ is a function of wavelength. The geometric extent of the cloud is also important, especially at short UV wavelengths [*Meyer et al., 1998*].

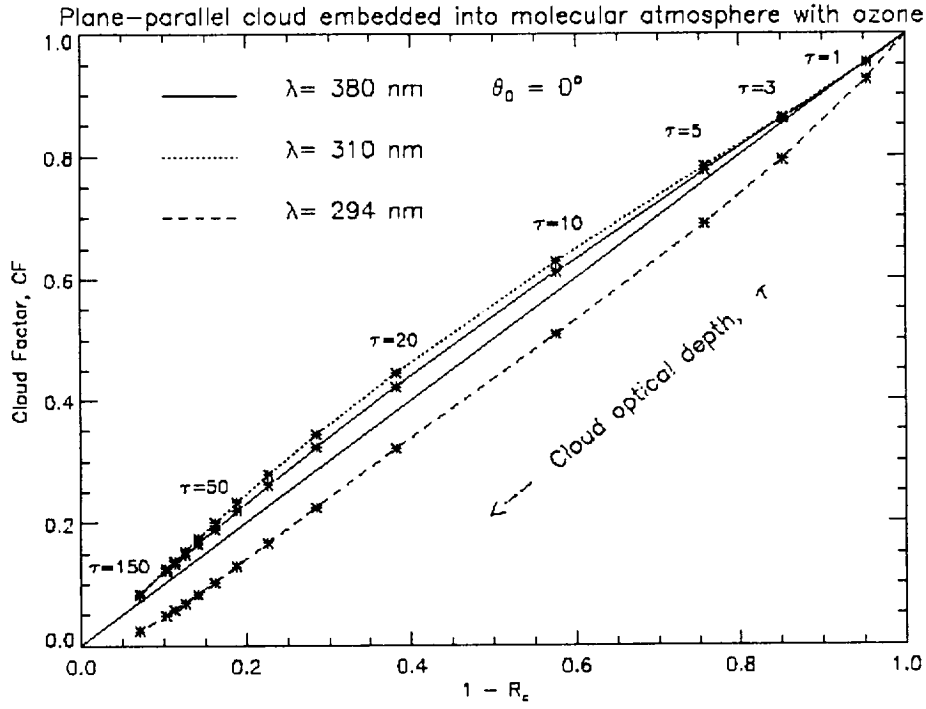

Figure 4 Relationship between C_T and cloud co-albedo for plane-parallel cloud embedded into molecular atmosphere with ozone. Wavelengths: 380nm (solid line); 310nm (dotted line) and 294nm (dashed line). $\theta = 0°$, $R_S=0$, and τ_C is a parameter..

2.2.3 C_T Dependence on Solar Zenith Angle

In the limiting case of visible wavelengths, one can neglect the effects of atmospheric scattering and ozone absorption, thus $C_T \sim (1-R_C) \sim 2\mu_0 / (\tau^* + 2\mu_0)$ (*i.e.*, C_T increases with increasing μ_0, *i.e.*, the maximum C_T is for overhead sun). For wavelengths where atmospheric-multiple scattering and absorption must be considered (UV-A and UV-B), multiple reflections between the cloud and molecular atmosphere effectively inhibit this dependence, so that C_T is a weak function of solar zenith angle. For $C_T(\lambda > 300nm)$, $dC_T/d\theta_o<0$ or approximately -6.7×10^{-4} for $\lambda = 310nm$, and for strongly ozone absorbing wavelengths ($\lambda<300nm$) the C_T dependence on solar angle is reversed, $dC_T/d\theta_o>0$ or approximately 5×10^{-4} per degree for $\lambda = 294nm$.

The sensitivity study conducted in this section has shown that for low surface albedo the cloud optical depth is the single most important parameter determining the value of C_T and the surface irradiance for overcast conditions. Since the C_T dependence on τ_C is approximately the same as the dependence of $(1-R_C)$ on τ_C (see Figure 4) for small solar zenith angles, $C_T(\theta_o<20°)$ can be approximated directly from the satellite estimation of cloud albedo without inferring cloud optical depth as an intermediate step. Second order effects (C_T spectral dependence and dependence on solar zenith angle) are well understood and can be captured from the

homogeneous cloud model. Therefore, for satellite estimation of UV transmittance through clouds, the problem of estimating C_T is reduced to the estimation of cloud hemispherical albedo at non-ozone absorbing wavelengths. In section 3 we will discuss this problem in detail.

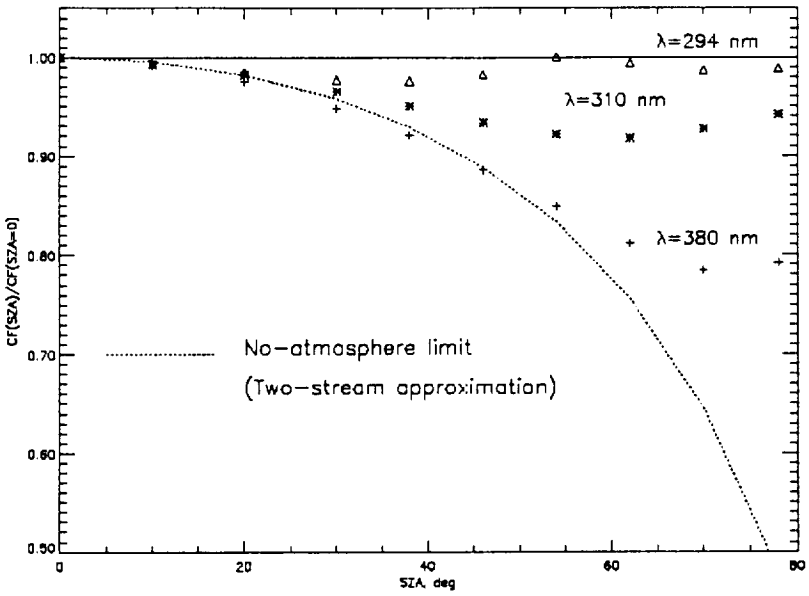

Figure 5 The dependence of C_T on θ_0.

3. Satellite Estimation of Cloud Factor C_T

In a satellite algorithm designed to estimate cloud albedo, R_C must be derived from measured backscattered radiances at the top of the atmosphere (TOA). To achieve this goal, three main problems should be considered:

- Subtraction of atmospheric(Rayleigh) backscatter above the cloud;
- Model of the angular (non-Lambertian) distribution of the radiation at TOA
- Subtraction of the surface reflectance from the total scene reflectivity.

Generally, the first and last problems are coupled. Fourteen years of TOMS radiance data and RT modeling have been used to develop a climatology of snow-free surface reflectivity [*Herman and Celarier*, 1997]. For low UV surface albedo typical of snow-or ice-free surfaces, or an optically thick cloud layer, one can neglect this coupling as a first approximation. In this section we consider two RT models developed to estimate cloud albedo over low-reflection surfaces ($R_S < 0.1$) from the satellite single-channel radiance measurements. The general case of highly reflecting surfaces will be considering in section 4. We start with discussion of the Lambert Equivalent Reflectivity (LER) model [*Eck et al.*, 1995] (Section 3.1). Next we discuss a single layer horizontally homogeneous cloud model (Section 3.2). Until Section 5 we consider strictly conservative cloud scattering (single scattering albedo $\omega_0 = 1$).

3.1 Lambert Equivalent Reflectivity Model

The backscattered radiance emerging from the top of atmosphere as seen by the satellite instrument, I_T, can be expressed as a sum of the atmospheric backscatter above the cloud, I_0 and the radiance reflected from the top of the cloud [*Chandrasekhar,* 1960; *Dave,* 1978; *Eck et al.*, 1987; *Eck et al.*, 1995; *Herman et al.*, 1996]:

$$I_T (\theta, \theta_0, ,P_c,R_T)= I_0 + R_T T(\theta, \theta_0,P_c)/[1- R_T S_b(P_c)] \quad (9)$$

where R_T is the Lambert Equivalent Reflectivity LER, S_b is the diffuse reflection of Rayleigh atmosphere illuminated from below by an isotropic source , θ is the satellite scan angle, T is the transmission function of a Rayleigh atmosphere, and P_c is the cloud-top pressure. For the wavelengths of interest, Io, S_b, and T are calculated assuming a purely Rayleigh atmosphere with no gaseous absorption and no Mie scattering. (A small correction is made for Rotational-Raman scattering, using the procedure described by *Joiner et al.*[1995]). P_C can be estimated from the monthly satellite cloud climatology data set as a function of location and season (International Satellite Cloud Climatology Project (ISCCP), *Rossow and Schiffer*, 1991).

Using R_T to estimate T_{CLOUD} assumes that the effect of clouds on the backscattered radiances in UV is similar to that of a Lambertian reflecting surface with enhanced albedo [*Eck et al., 1987;Eck et al.,* 1995; *Herman et al.*, 1996; *Krotkov,* 1997]. It should be stressed that the R_T is calculated for each scanning direction to fit the satellite measured radiance. If the cloud reflects radiation isotropically, the R_T would be the true cloud hemispherical albedo, $R_T = R_C$. In general, clouds are non-Lambertian reflectors (*e.g.*, for empirical ERBE angular dependence models see *Suttles et al.* [1989]).

Because of the angular-dependent reflectance of the clouds systems, R_T is a function of the satellite zenith angle, θ, solar zenith angle, θ_0, and the azimuthal angle, φ. For a clear scene, R_T is close to the ground plus tropospheric aerosol reflectivity, which is uniformly low $R_S<0.1$) in the UV spectral region [*Eck et al.*, 1987; *Herman and Celarier*, 1997].

In an earlier work [*Eck et al.*, 1995], it was assumed that the UV reflectivity, R_T, measured by the Total Ozone Mapping Spectrometer (TOMS) is representative of the cloud hemispherical albedo with a small correction for the underlying surface reflectivity so that R_T-R_S could be used to estimate the C_T.

Figure 6 shows the relationship between R_T at 380nm and the cloud hemispherical albedo, R_C (see Equation 1) for a 1 km thick cloud embedded in a mid-latitude ozone containing atmosphere, zero surface albedo, and typical Nimbus-7/TOMS scanning geometry (Figure 6a shows nadir- and Figure 6b the 54^o (azimuth 90^o) viewing directions). The results show that although there is a general correlation between $R_T = R_{380}$ and Rc, these quantities are not the same. The differences between Rc and R_T depend on the viewing geometry, particularly the solar zenith angle

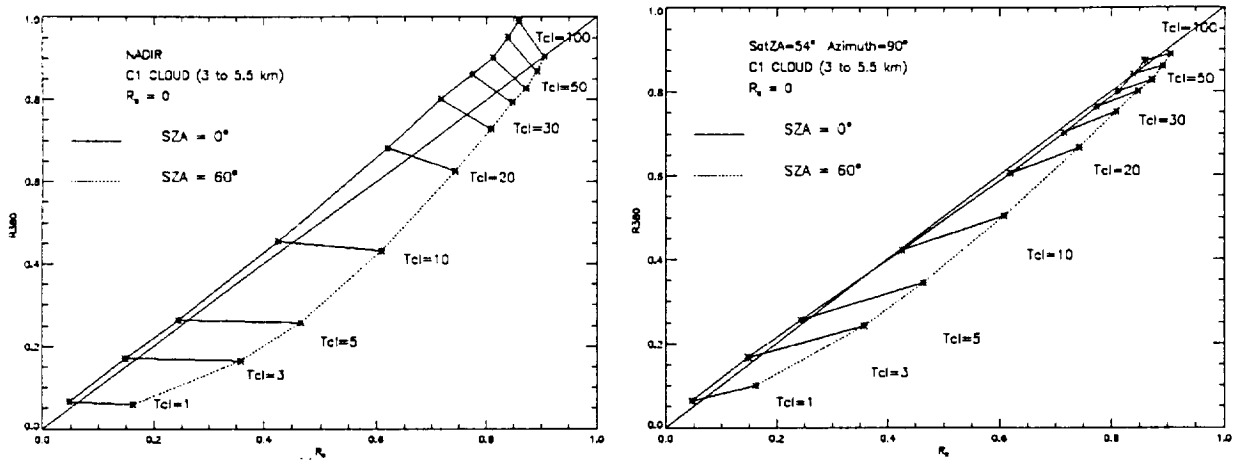

Figure 6 R_{380} **vs** R_C , $\theta_o=0^o$ **(solid line) and** $\theta_o=60^o$ **(dotted line). a) Left Panel: nadir observational direction** $\theta=0°$**; b) Right Panel:** $\theta=54°$; $\varphi=90°$.

Estimates of C_T with this method are most accurate for the Nimbus-7 TOMS mid-latitude scanning geometry (TOMS overpass near local noon and the instrument scan nearly perpendicular to the principal plane of the sun), which minimizes the effects of cloud anisotropic angular reflectance (Figure 6b). However, for other conditions (high latitudes), the failure to account for angular dependence of the backscattered radiation field can lead to large errors in this method. For common observing conditions the errors can be 20% or more.

Neglecting the surface reflectivity R_S is justified in the case of the optically thick clouds (Rc > 0.5). For optically thin clouds over a low-reflectance surface, a simple correction for the underlying surface contribution was proposed [*Eck et al.*, 1995]:

$$R_{ECK} = (R_{380} - Rs)/ (1-2Rs)$$

$$C_{ECK} = 1 - R_{ECK}, \qquad R_{380} < 0.5 \tag{10}$$

$$C_{ECK} = 1 - R_{380}, \qquad R_{380} > 0.5$$

where R_S is based on minimum R values measured by Nimbus-7/TOMS [*Eck et al.*, 1995; *Herman and Celarier*, 1997].

The simple R_{380}-LER method was compared with measurements at Toronto, Canada for mid-latitude observational conditions using direct comparisons with the ground based Brewer #14 UV irradiance measurements [*Eck et al.*, 1995]. Reanalysis of this data [*Herman et al.*, 1998] showed that there is a 20% disagreement (TOMS estimates greater than Brewer measurements) even though estimates of UV irradiance are made near local noon with the TOMS instrument scanning nearly perpendicular to the principal plane of the sun. The 20%

disagreement includes C_T errors in addition to other systematic instrument or aerosol related errors.

3.2 Plane-parallel cloud model

To implement an improved cloud correction compared to Equation10, detailed radiative transfer calculations were done to calculate the downward irradiance at the ground, and the upward radiances at the top of the atmosphere, using a midlatitude 325 DU ozone profile and a homogeneous Diermendjian [1969] "C-1" type cloud located between 3.5 km and 5.0 km. The calculations were conducted with cloud-optical thicknesses from 0 to 100, surface reflectivities from 0 to 1, surface heights of 0 and 3.5 km, and solar zenith angles from 0 to 88°. Upward radiances were post-processed into effective cloud optical depth [*Krtokov et al., 1997; Herman et al., 1998*].

We should stress, however, that TOMS UV technique does not rely on retrieval of the real cloud optical thickness (*i.e.*, total column water content). The effective τ_{eff} derived from TOMS radiances would be equal to the real τ_C only in the idealized case of a plane-parallel horozontally-homogeneous cloud layer. In the real case, τ_{eff} becomes a function of the assumed surface reflectivity, TOMS observational geometry, cloud fraction, and solar zenith angle. Neglecting cloud fraction, a lookup table for C_T was built that gives $\tau_{eff}(\theta_o, R_T, R_S)$. The value of R_S was taken from a climatological database that was developed using the 15 years of TOMS data [*Herman and Celarier,* 1997]. As a final step, a Lagrange interpolation was used to determine the C_T between the tabulated parameter values using the τ_{eff} as a parameter.

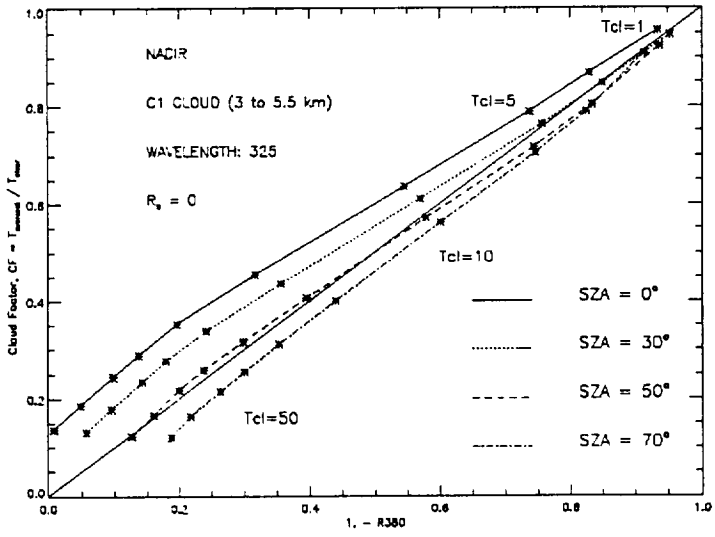

Figure 7. Cloud transmittance factor, C_T at 325nm as a function of the 380nm Lambert Equivalent Reflectivity R380, for solar zenith angles between 0^o and 70^o, derived from TOMS backscattered radiance.

Figure 7 shows C_T at 325 nm as a function of (1- R_{380}) for a 1-km thick cloud embedded into a mid-latitude ozone containing atmosphere at 5 km altitude. Compared to (1-R_{380}), the values of C_T are about 20% larger for thick clouds (τ_c>10) and θo less than ~ 40°. Similar calculations at different measurement geometries (see *Herman et al.*, 1998) indicate that equation (10) can be used to estimate C_T to about 10% - 20% accuracy for snow-free conditions. Since the LER model does not give the spectral dependence of C_T (see Figure 2), the LER method would underestimate C_T at biologically important UV-B wavelengths (*e.g.*, 310nm).

3.3 Comparisons with Ground-Based Data Sets

Satellite data represent instantaneous radiance measurements averaged over the large geographical extent in the footprint (the TOMS footprint is on average 100 km by 100 km). Because of high cloud variability and different FOV between ground and satellite instruments, only time-averaged irradiances should be compared to ground-based measurements. The period of averaging should be at least a week in order to minimize the effects of local cloud changes. *Herman et al.* [1998] compared the 7 days running averages of the daily TOMS estimated UV-irradiances with corresponding 7-day running averages of the daily Brewer (#14) irradiances in Toronto (obtained within ±30min of TOMS overpass time). They found that during the summertime the TOMS estimated irradiances are larger by about 20% than those measured by Brewer spectrometer. These differences represent the combined effect from different cloud and aerosol conditions including calibration uncertainties of both instruments [*Herman et al.*, 1998].

An alternative approach is to group the measurements according to satellite reflectivity data and compare the average irradiances for each reflectivity range. Comparing only cloud factor data C_T (after normalizing the irradiance by the clear sky irradiance) reduces the instrument-calibration bias (mainly the cosine correction [*Krotkov et al.*, 1998]), to the extent that it is the same for clear and cloudy conditions. This method is useful for understanding differences between the satellite algorithm and ground-based measurements for varying cloud amounts and corresponding average reflectivity in the TOMS FOV.

The daily TOMS estimates of C_T (sections 3.1 and 3.2) were compared with ground-based Brewer spectrometer measurements of the same quantity. The Brewer spectra were measured at Toronto between 1989 and 1998 by instrument #14. The comparisons were done under conditions without snow or ice (May through September data). The Brewer cloud factor (C_{TB}) was obtained by dividing the measured irradiance at 324 nm by "statistical clear sky" Brewer-irradiance parameterization [Fioletov 1997]:

$$T_{CLEAR}(324) = -0.119848 - 0.0239033\,\theta - 0.00124988\,\theta^2 + 0.000274423\,\theta^3 - 1.5479E\text{-}005\,\theta^4 + 4.20862E\text{-}007\,\theta^5 - 6.10836E\text{-}009\,\theta^6 + 4.54795E\text{-}011\,\theta^7 - 1.36825E\text{-}013\,\theta^8 \quad (11)$$

where θ is the solar zenith angle in degrees. The parameterization is based on a 95-percentile method: when the measured irradiance data (after the Earth-Sun distance adjustment) are compared to this formula, for each solar zenith angle approximately 95% of all data are less than $T_{CLEAR}(324)$ and 5% are more than $T_{CLEAR}(324)$.

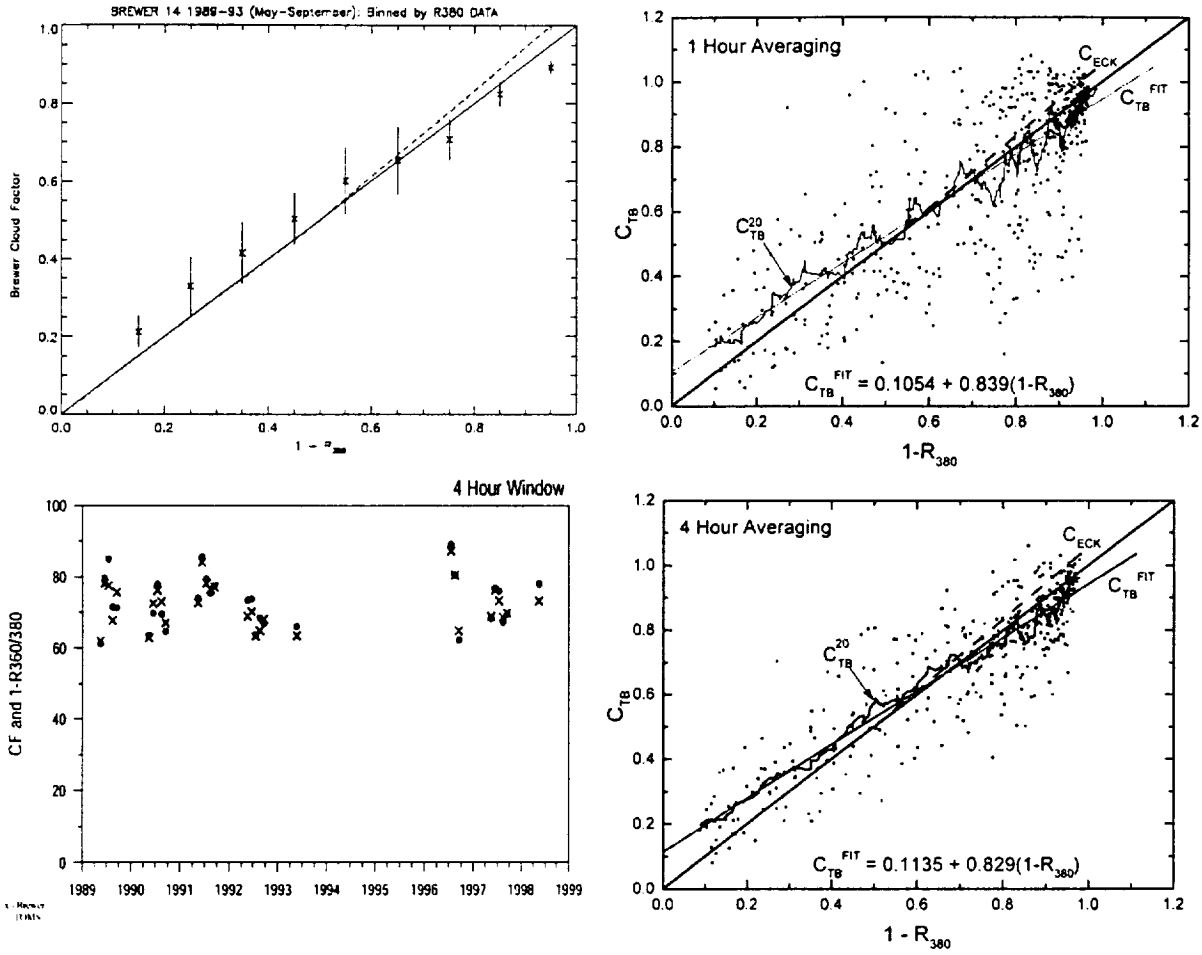

Figure 8 Brewer #14 measured C_{TB} versus TOMS measured R_{380} from daily measurements in Toronto during May to September, 1989-1993. a) The left panel shows the results of reflectivity binning, and b) the right panel shows a 20-point running average to the data sorted by reflectivity C^{20}_{TB} and a the linear least squares fit to the data points C_{TB}^{FIT}. The dashed line is $X=C_{ECK}=1-(R_{380}-0.05)/0.9$ [*Eck et al., 1995*].

For Toronto during May to September θ is between 20° and 50° for the near-noon TOMS overpass times. The new cloud factor C_T, shown in Figure 7 (TOMS nadir view), is larger than $1-R_{380}$ for cloudy skies ($R_{380} > 0.5$) and approaches $1-R_{380}$ as R_{380} becomes small (near R_S) . For cloudy skies C_T is similar to C_{TB}, but $C_T > C_{TB}$ for nearly clear skies. The clear sky discrepancy has been interpreted in terms of absorbing aerosols that are seen by the Brewer instrument, but

not by TOMS [*Krotkov et al., 1998; Herman et al., 1998*]. The presence of absorbing aerosols would make $C_{TB} < 1$ when R_{380} becomes small.

The Brewer measured C_{TB} data (measured within ±30 of TOMS overpass time) were binned using 10% intervals of TOMS R_{380}, to calculate means and standard deviations. The mean Brewer C_{TB} values for each R_{380} bin are shown in Figure 8a. The error bars are $\pm 2\sigma$ (σ is the standard error of the mean) for each bin. Running averages of C_{TB} and a least squares fit to the data points are shown in Figure 8b (1-hour average) and 8d (4-hour average). The dashed line shows the reflectivity-based TOMS estimated cloud correction factor for surface reflectivity 0.05 [see Equation 10 and *Eck et al 1995*]. For both 1-hour and 4-hour cases, TOMS overestimates C_T for broken and thin clouds ($R_{380} < 0.3$), but underestimates for thick clouds ($R_{380} > 0.45$). The running average C_{TB}^{20} shows that the slope of the least squares fit is locally meaningful and not determined by the large cluster of points where R_{380} is near 1.

Figures 8b and 8d show that C_{ECK} overestimates C_T for broken and thin clouds ($R_{380} < 0.3$), but underestimates for thick clouds ($R_{380} > 0.45$). At least part of the Eck et al [1995] underestimation for thick clouds is due to neglecting of C_T spectral dependence (see section 2.2.1), which has been recently incorporated into the current TOMS cloud correction algorithm (see figure 5 where the difference between the C_{ECK} and current TOMS C_T [*Krotkov et al., 1997; Herman et al 1998*] is shown).

Figure 8 shows that R_{380} provides an estimation for C_{TB} with some systematic bias, and that the random error of any single measurement is large (see Figure 8b). The random error results mainly from the fact that one compares the spatially averaged satellite data with a single-point ground measurement under highly variable cloud conditions. However, Figure 8 also shows that the random error can be reduced by considering averages over reflectivity bins or by using running averages (this is similar to the effect obtained using weekly averaging [*Herman et al., 1998*]). The remaining differences are systematic and represent the bias of particular satellite cloud correction algorithm

Brewer measurements and TOMS irradiance estimates are based on different cloud amounts in their respective fields of view. For example, when R_{380} is small, the sky is most likely to be filled with a mixture of clear and cloudy regions. At the TOMS overpass time the Brewer instrument can measure an irradiance value that is greater or less than the TOMS value with nearly equal probability. Increasing the time over which the Brewer data are averaged increases the likelihood that the average cloud amount in the TOMS and Brewer scenes are similar. This can be seen by comparing Figures 8b and 8a. Figure 8b contains 1 measurement per point and 8d contains 4 Brewer measurements that are averaged to produce 1 data point. For low R_{380} the spread of C_{TB} about the $1 - R_{380}$ is significantly reduced in the 4 hour average case (Figure 8d). Standard deviations are 37%, 26%, and 21% for 1-hour, 2-hour and 4-hour averaging, respectively. A 6-hour average has larger standard deviations then the 4 hour average because the difference in time between Brewer and TOMS measurements is too large.

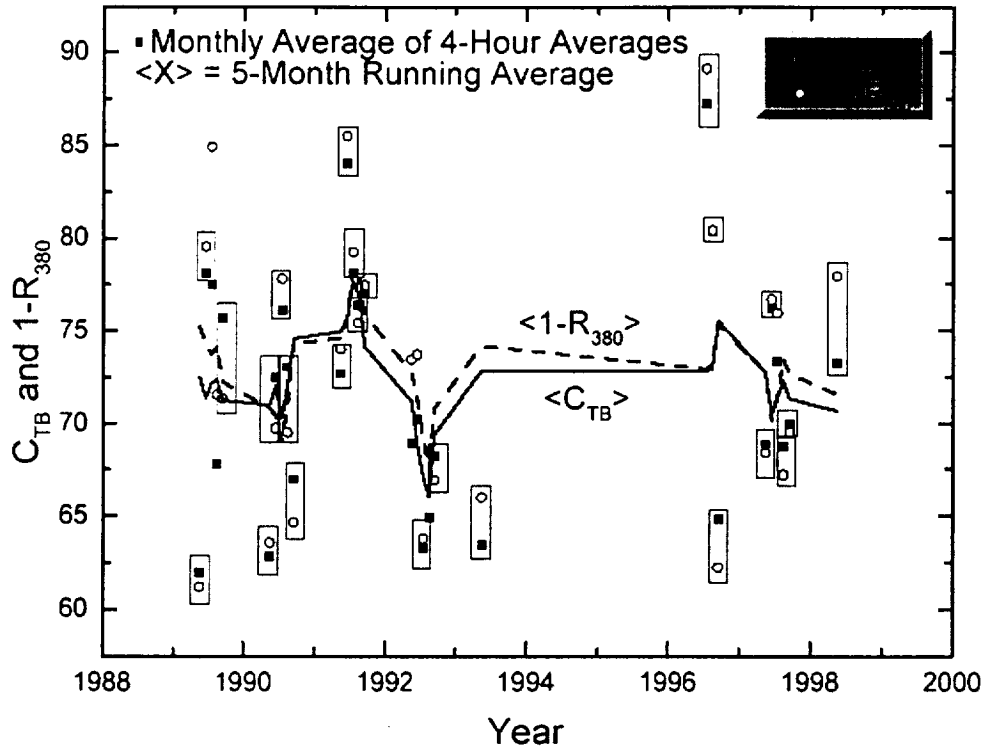

Figure 9 A comparison between monthly averages of 4-hour daily averages of the Brewer C_{TB} and the TOMS 1-R_{380} [▪ ○], and a comparison between 5-month running averages <X>. The boxed symbols [▪ ○] are averages for the same month that are close in value.

When the 4-hour daily data are combined into monthly averages (see Figure 9), the agreement between the TOMS and Brewer estimated cloud transmittances is improved (each pair of points within a box is for the same month). The data used are for the period 1989 to June 1998 and are from both Nimbus-7/TOMS (1979 to May 1993) and Earth-Probe/TOMS (August 1996 to present). For most months the agreement is sufficiently close to be useful for calibration of the ground-based Brewer system. Since some months are too much in disagreement for calibration purposes, it is recommended that running averages of the monthly averages be used. Here the agreement is within a few percent, well below the instrument to instrument uncertainty (10 to 20%).

4. Clouds Over Snow

The UV and visible reflectivity of fresh snow can be extremely high: $R_S > 0.95$ [*Bohren and Barkstorm* 1974; *Wiscombe and Warren* 1980; Grenfell et al., 1994; *Zege and Kokhanovskii*, 1997; *Herman et al.*, 1998]. Therefore, the possible errors in satellite-C_T estimation due to surface-albedo uncertainty differ significantly for winter and summer conditions. Here we consider the case of conservative cloud scattering, but allow arbitrary surface albedo, Rs. The basic behavior of the cloud-surface system can be understood while neglecting atmospheric scattering. This approximation is useful for $\lambda \geq 360$ nm where the atmospheric scattering effects

are small. Including the atmosphere causes the $1-R_{SYSTEM}$ lines to be replaced with curved lines (see Figure 4). In addition, R_{SYSTEM} can be greater than 1 for some observing angles. This effect is observed in the TOMS data.

For arbitrary R_S and neglecting atmospheric effects, C_T can be expressed as a solution of the Stokes problem (Equation 3). The albedo of the cloud-surface system, R_{SYS} , can be calculated from the energy balance:

$$R_{SYS} = R_C + T_C R_S T^* / [\, 1 - R_S R_C^{Dif} \,] \qquad (12)$$

where $T_C = 1 - R_C$ and $T^* = 1 - R_C^{Dif}$ are cloud transmittance of direct and diffuse radiation for a black underlying surface. Equations (3) and (12) present a formal relationship between C_T and albedo of the system for arbitrary R_S. (See Figure 2 and Equation 4 for values of R_C^{Dif}).

Figure 9 illustrates the relationship between C_T, R_{system} and R_S for a homogeneous plane-parallel cloud model for $\theta=0°$ and $60°$ in the absence of a scattering atmosphere. C_T was calculated directly from its definition (Equation 2) for different values of surface albedo using the DISORT radiative transfer program. The diagram confirms our qualitative conclusions and allows quantitative C_T estimation for any combination of R_{SYSTEM} and R_S. It is quite obvious that in the presence of snow ($Rs>0.3$) one needs to know both measured reflectivity R_{SYS} and surface albedo R_S, to estimate C_T (even for thick clouds, $\tau_C>30$). These two independent quantities cannot be estimated from a single channel satellite reflectivity.

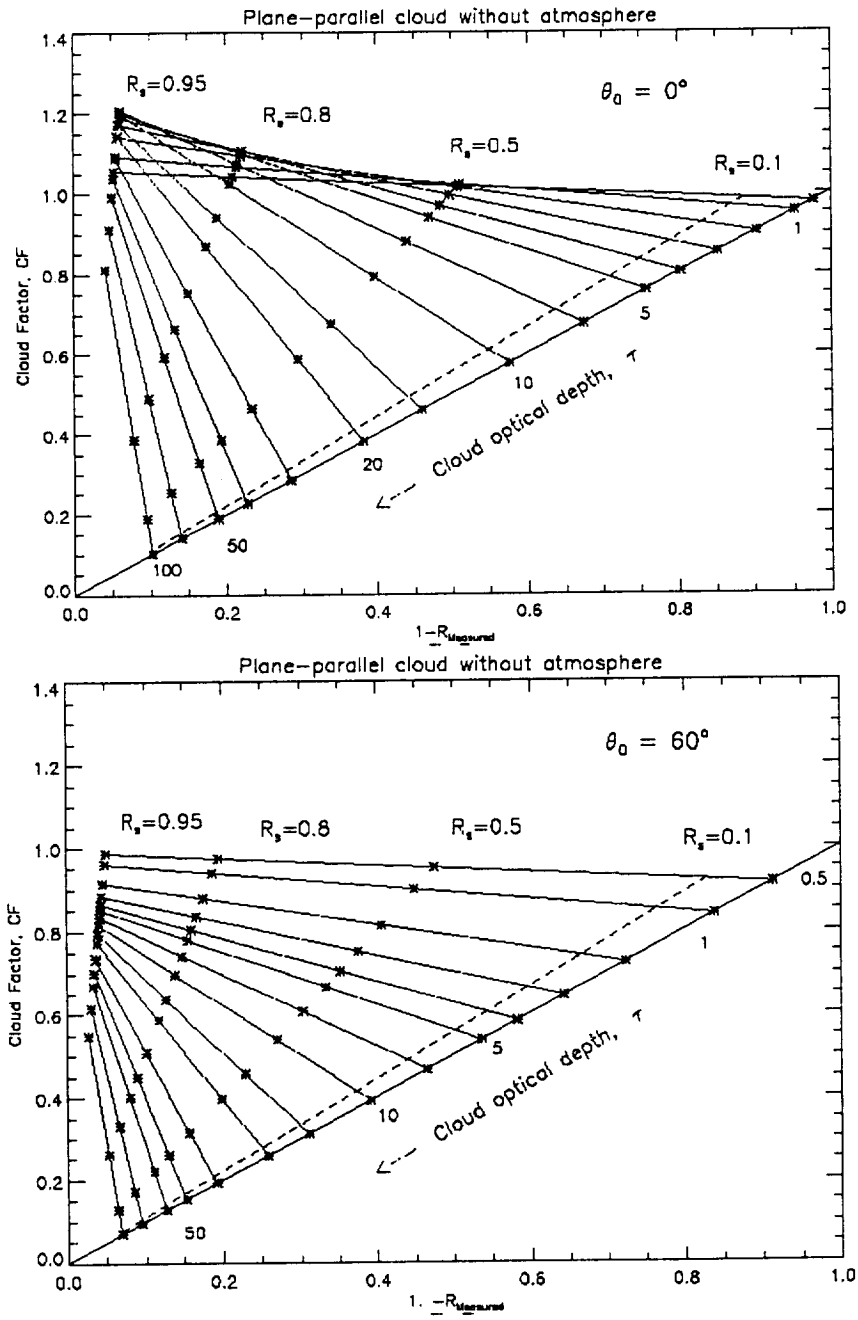

Figure 9 The relationship between the total Cloud Factor C_T and co-albedo of the "cloud-surface" system, $1-R_{system}$ using DISORT [*Stamnes et al.*, 1988] for a conservative cloud layer [C1, Deirmendjian, 1969] over a Lambertian reflective surface with reflectivity R_S between 0 and 0.95 (fresh snow). a: Top) Overhead sun: θ_0=0; b: Bottom) θ_0=60°

For TOMS, the best that can be done for estimating UV transmittance through clouds over snow/ice, in the absence of independent information, is to use a climatology for estimating R_S. The faction of the measured reflectivity associated with a possible cloud is assigned on a probabilistic basis. For example, in a suburban area with trees and buildings, the surface reflectivity over a region of 100x100 km^2 (TOMS FOV) rarely exceeds 0.4 when there is snow on the ground (except immediately after a fresh snowfall). Measured reflectivities in excess of a threshold value could be assigned to an overlying cloud layer. For estimation of UV irradiance, averaging the transmittance over at least a week should minimize errors caused by fresh-snow conditions compared to the true weekly dosage.

For fresh snow (Rs>0.5) and $\tau<50$ and overhead sun the irradiance at the surface exceeds that for a clear atmosphere (Figure 9a) [*see also Shettle and Weinman, 1970*]. If $Rs > Rc/R_C^{Dif}$, then $C_T>1$ (see Equation 3 and Section 2.1). Using a two-stream approximation for Rc (see Equation 5), the condition $C_T>1$ can be expressed as:

$$R_S > 2[(\tau^*+2\mu_o)\ln(1+2/\tau^*)]^{-1} \quad (13)$$

From this equation one can see that a combination of low solar-zenith angle ($\mu o\sim1$) and high surface albedo is required for enhanced cloud transmittance ($C_T>1$). In this regime the cloud layer becomes more transparent from above (direct solar radiation) than from below (diffuse illumination by the snow surface). Therefore, photons are "trapped" between the surface and the cloud bottom ("cavity" effect). The cloud optical depth can vary in a wide range (*e.g.*, τ_C =1 to 50). We note that $C_T>1$ regime does not violate energy conservation, which can be written in the form:

$$C_T(1-R_S)= R_{system} \quad (14)$$

The condition of low solar-zenith angle ($\mu o\sim1$) is critical. As can be seen from Figure 9b, the enhanced transmittance ($C_T>1$) does not occur for $\mu_O=0.5$ ($\theta o=60^O$). Also, optically thick clouds eventually reduce C_T to less than unity ($\tau>50$).

5. Non-Conservative Cloud Scattering

In the satellite estimation of cloud transmittance in the visible and near UV spectral regions ($\lambda \geq 360$ nm), a conservative-scattering regime is usually assumed ($\omega=1$) . Calculations [*Twomey, 1972; Twomey and Bohren, 1980; Twohy et al., 1989; Chylek et al., 1996*] and direct measurements [*King et al., 1990*] of the cloud single-scattering albedo ω show that this is a reasonable assumption for clean marine clouds ($\omega>0.9999$). Yet other measurements (although not direct) estimate $\omega < 0.999$ at 0.4μm [*Melnikova et al.,* 1997]. In this section we extend our analysis to the case of slightly non-conservative cloud scattering (which might be the case for a mixture of clean-water droplets with absorbing aerosols such as those containing soot). Since we are considering wavelengths where scattering effects are not important, we neglect the atmosphere in the model calculations.

Figure 10 is similar to Figure 9 except the cloud scattering is assumed slightly non-conservative (ω=0.999). We note that differences are not large for small $\tau < 10$ and low surface reflectivity (R_S<0.1). However, the general relationship between C_T and R_{system} is quite different from conservative case (Figure 9a). For example, for low R_S<0.1, R_{system} increases with τ_C, but never gets larger than ~80% even for τ_C>100. In other words, even very thick ω=0.999 clouds do not appear as bright as thinner ω=1 clouds. On the other hand , over fresh snow surfaces, the reflectivity of the scene decreases with increase in cloud optical thickness because of multiple reflections and losses within the cloud. For R_S~0.8, R_{system} does not change with τ_C, but C_T does (Rsystem~0.8 while C_T changes from 1.1 to zero with increase in τ). Thus, the satellite reflectance measurements are not useful for determining C_T for R_S>0.5 even if R_S is known a-priori. Enhanced cloud transmittance regime (C_T>1) is still possible even for slightly non-conservative cloud scattering. We have shown that even slight absorption makes it impossible to estimate C_T over bright snow surfaces from satellite reflectance measurements.

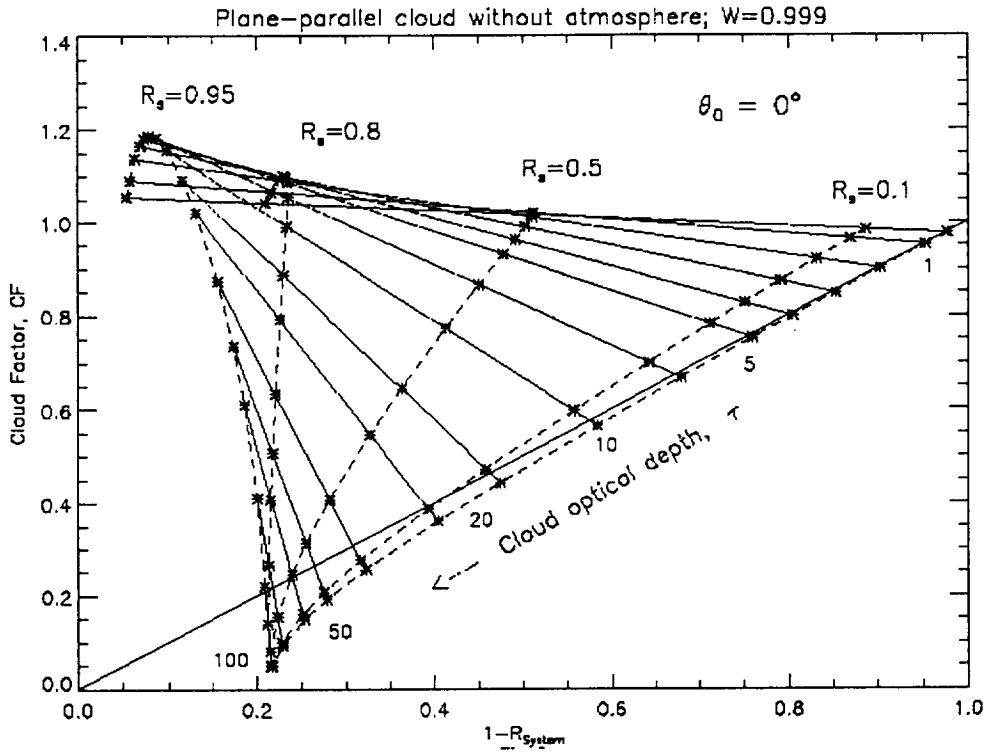

Figure 10 Similar to Figure 9a but for non-conservative scattering, ω_o=0.999

Although the details are not shown in this paper, the spectral dependence of a slightly absorbing cloud is quite different than for the case where ω_o=1.

6. Summary

Radiative transfer calculations have been presented for the convenient estimation of the transmission T of ultraviolet radiation through plane parallel clouds over a surface with reflectivity R_S. For snow-free surfaces and conservative-cloud scattering it was demonstrated that the transmittance of a cloudy atmosphere can be approximated from the satellite measurements of reflectivity R_C at non-absorbing UV wavelengths as 1- (R_C - R_S) with an error of about 20%. The amount of error depends most strongly on the solar zenith angle and optical depth. At this level of approximation, the TOMS R_{SYS} measurements can be utilized directly to approximate cloud albedo, cloud transmittance or C_T, and the irradiance at the Earth's surface.

A better approximation to C_T can be obtained from an atmospheric radiative transfer RT model with homogeneous-cloud layer to convert satellite measured radiance to cloud transmittance using a table look-up method. The RT method predicts larger cloud transmittances than the 1- (R_C - R_S) method for solar zenith angles $\theta_o < 50°$, and accounts for the spectral dependence of the cloud factor C_T. Radiative transfer calculations show that the effects of cloud anisotropic reflectance from non-Lambertian surfaces are reduced in the plane perpendicular to the solar-principal plane. This is the geometry appropriate for the near-noon radiance measurements obtained from TOMS.

The cloud transmittance function C_{TB} has been derived from Brewer #14 data in Toronto, Canada for May to September 1989 - 1993 and compared to the satellite estimations of C_T. As expected, the day to day variations in reflectivity are too large to be directly compared to C_T. When the Brewer data are averaged in time or in reflectivity bins it has been shown that C_{TB} is close to 1-R_C and that there are 20% systematic differences relative to 1-R_C for clear and cloudy conditions.

For TOMS estimates of UV irradiance in the presence of both snow and clouds, independent information about snow albedo is needed for conservative cloud scattering. However, for nonconservative cloud scattering (*e.g.*, ω=0.999) with snow reflectance above 0.5, the satellite measured scene reflectance cannot be used to estimate surface irradiance. Adding atmospheric scattering to the model does not change this conclusion. For low solar-zenith angles and high surface albedo, enhanced cloud transmittance is possible (C_T>1).

7. References

Ahmad, Z. and Frazer, An iterative radiative transfer code for ocean-atmosphere systems, *J. Atmos. Sci.*,**39**, 656-665, 1982.

Bates, D.R., Rayleigh Scattering by Air, *Planet. Sp. Sci.*, 32, 785-790, 1984.

Bass, A.M., and R.J.Paur, The ultraviolet cross-sections of ozone, I, Measurements, in Atmospheric Ozone, in Ozone Symposium (1984:Halkidiki, Greece): Atmospheric Ozone, edited by C.Z.Zeferos, and A.Ghaz, p.606-616, D.Reidel, Hingham, Mass., 1985.

Bohren, C.F. and B.R.Barkstorm, Theory of the Optical Properties of Snow, *J. Geophys. Res.*,**79**, 4527-4535, 1974.

Chandrasekhar, S. (1950) Radiative Transfer, Oxford Univ. Press, UK; republished by Dover, N.Y., USA, 393p., 1960

Chylek, P., et al., Black carbon and absorption of solar radiation by clouds, *J.Geophys. Res., 101, 23365-23371, 1996.*

Coakley , J.A.Jr., and P.Chylek, The two-stream approximation in radiative transfer: Including the angle of the incident radiation, *J. Atmos. Sci.*, 32,409-418, 1975.

Dave, J.V., Effect of aerosols on the estimation of total ozone in an atmospheric column from the measurements of its ultraviolet radiance, *J. Atmos. Sci.*,35, 899-911, 1978

Deirmendjian, D., Electromagnetic scattering on spherical polydispersions, N.Y., American Elsevier Pub. Co., 290p., 1969.

Eck, T.F., P.K.Bhartia, P.H.Hwang, and L.L.Stowe, Reflectivity of Earth's surface and clouds in ultraviolet from satellite observations, *J. Geophys. Res.*,**92**, 4287-4296, 1987.

Eck, T.F., P.K.Bhartia, and J.B. Kerr, Satellite Estimation of spectral UVB irradiance using TOMS derived ozone and reflectivity, *Geophys. Res. Lett.*, **22**, 611-614, 1995.

Fioletov V.E. and W.F.J. Evans, The influence of ozone and other factors on surface radiation, *In: Ozone Science: a Canadian Perspective on the changing ozone layer*, Edited by D.I.Wardle, J.B.Kerr, C.T. McElroy, and D.R. Francis, CARD 97-3, Atmospheric Environment Service (AES) Report, 4905 Dufferin Street, Downsview, Ontario M3H 5T4, Canada, pp. 73-90, 1997.

Frederick, J.E., and D. Lubin, The budget of Biologically active ultraviolet radiation in the Earth-Atmosphere system, *J. Geophys. Res.*,**93**(D4), 3825-3832, 1988.

Frederick, J. E. and C. Erlick, The attenuation of sunlight by high latitude clouds: Spectral dependence and its physical mechanisms, *J. Atmos. Sci., 54*, 2813-2819, 1997.

Grenfell, T. C., S. G. Warren, and P. C. Mullen, Reflection of solar radiation by the Antarctic snow surface at ultraviolet, visible, and near-infrared wavelengths, *J. Geophys. Res., 99*, 18,669-18,684, 1994.

Herman, J.R., N.A.Krotkov, E.Celarier, D.larko, and G.Labow, The distribution of UV radiation at the Earth's Surface from TOMS measured UV-Backscattered Radiances, submitted to *J. Geophys. Res.*, 1998.

Herman, B. M. and S. R. Browning,, A numerical solution to the equation of radiative transfer, *J. Atmos. Sci., 22*, 559-566., 1965.

Herman,J. R., P. K. Bhartia, J. Kiemke, Z. Ahmad, and D. Larko, UV-B increases (1979-1992) from decreases in total ozone, *Geophys. Res. Lett., 23*, 2117-2120, 1996.

Herman, J.R. and E. Celarier, Earth Surface Reflectivity Climatology at 340 nm to 380 nm from TOMS Data, J. *Geophys. Res., 102*, 28,003 - 28,011, 1997.

Joiner, J., P.K.Bhartia, R.C.Cebula, E.Hilsenrath, R.D.McPeters, and H. Park, Rotational Raman scattering (Ring effect) in satellite backscatter ultraviolet measurements, *Appl. Optics*, **34**,4513-4525, 1995.

King, M.D., and Harshvardhan, Comparative accuracy of selected multiple scattering approximations, J. Atmos. Sci., 43,784-801, 1986.

King,M.L., L.F.Radke, and P.V.Hobbs, Determination of the spactral absorption of solar radiation by Marine Stratocumulus clouds from airborne measurements within clouds, *J.Atmos.Sci.*,**47**, *894-907, 1990.*

Krotkov, N.A., P.K. Bhartia, J.R. Herman, V. Fioletov and J. Kerr "Satellite estimation of spectral surface UV irradiance in the presence of tropospheric aerosols 1: Cloud-free case" *J. Geophys. Res., 103*, 8779-8793, 1998.

Krotkov N.A., P.K.Bhartia, J.Herman, E.Celarier, and T.Eck, Estimates of spectral UVB irradiance from the TOMS instrument: effects of clouds and aerosols, In: *IRS'96: Current Problems in Atmospheric Radiation*, Eds. W.L.Smith and Knut Stamnes, A.DEEPAK Publishing, 873-876, 1997.

Lenoble, J., Atmospheric radiative transfer , A.Deepak Publishing , Hampton, VA, 532p.,1993.

Liou, K.N., Radiation and cloud processes in the atmospere, Oxford University press, 487p., 1992.

Lubin D., P.Ricchiazzi, C.Gautier, and R.H.Whritner, A Method for Mapping Antarctic surface ultraviolet radiation using multispectral satellite imagery, *In: Ultraviolet Radiation in Antarctica: measurements and biological effects*, Weiler, C.S., and P. A. Penhale, Eds., AGU, *Antarctic Research series*, **62**, 53-82, 1994.

Lubin, D., E.H.Jensen, and H.P. Gies, Global surface ultraviolet radiation climatology from TOMS and ERBE data, *J.Geophysical Research*, 103, 26061-26091, 1998.

Madronich, S., Implications of recent total ozone measurements for biologically active ultraviolet radiation reaching the Earth's surface, *Geophys. Res. Lett.*, **19**, 37-40, 1992.

Madronich, S.,The atmosphere and UV-B Radiation at ground level, *In Environmental UV Photobiology, edited by* A. R.Young et al., Plenum Press, New York, pp.1-39, 1993.

Mayer,B., A.Kylling, S.Madronich, and G.Seckmeyer, Enhanced Absorption of UV Irradiance due to Multiple Scattering in Clouds: Experimental Evidence and Theoretical Explanation, accepted BY *J.Geophys. Res*, 1998.

McKenzie, R. L., M. Kotkamp, and W. Ireland, Upwelling UV spectral irradiances and surface albedo measurements at Lauder, New Zealand, *Geophys. Res. Lett., 23*, 1757-1760, 1996.

McPeters, R. D., S. M. Hollandsworth, L. E. Flynn, J. R. Herman, and C. J. Seftor, Long-term ozone trends derived from the 16-year combined Nimbus 7/Meteor 3 TOMS Version 7 record, *Geophys. Res. Lett., 23*, 3699-3702, 1996.

Melnikova,I.N. and Mikhailov, V.V. Spectral Scattering and absorption coefficients in Strati derived from Aircraft Measurements, *J.Atmos.Sci.*,**51**, 925-931, 1994.

Meerkoetter, R.B., Wissinger, and G.Seckmeyer, Surface UV from ERS-2/GOME and NOAA/AVHRR data: A case study, Goephys. Res.Lett., 24, 1939-1942, 1997.

Nack M.L. and Green A.E.S., Influence of clouds, haze and smog on the middle ultraviolet reaching the ground, Appl. Optics, v13, N10, pp.2405-2415, 1974.

Determination of cloud layer optical parameters from measurements of reflected and transmitted solar radiation, *Izvestia, Atmospheric and Oceanic Physics*, v.10, 7, 1997.

Rossow, W.B. and R.A.Schiffer, ISCCP cloud data products, *Bull. Am. Meteorol. Soc.* **72**, pp.2-20, 1991.

Rublev, A.N., A.N.Trotsenko, N.E.Chubarova, O.M.Isakova, I.V.Geogdzhaev, T.V.Kondranin, P.Yu. Romanov, The use of satellite data for determination of downward solar radiation fluxes at cloudy conditions and their comparison with ground-based measurements, *IRS'96: Current Problems in Atmospheric Radiation*, W. Smith and K. Stamnes (Eds), pp. 488-491, 1997

Seckmeyer, G., B. Mayer, G. Bernhard, R. Erb, A. Albold, H. Jäger, and W. R. Stockwell, New maximum UV irradiance levels observed in Central Europe, *Atmos. Environ., 31*, 2971-2976, 1997.

Stamnes, K., S.C. Tsay, W. Wiscombe, and K. Jayaweera, Numerically stable algorithm for discrete-ordinate-method radiative transfer in multiple scattering and emitting layered media, *Appl. Opt., 27*, 2502-2509, 1988.

Shettle, E.P., and J.A.Weinman, The Transfer of Solar Irradiance through inhomogeneous turbid atmospheres evaluated by Eddington's approximation, *J. of Atmosp. Sciences,* 1048-1055, 1970

Suttles, J.T., R.N.Green, G.L.Smith, B.A. Wielicki, I.J.Walker, V.R.Taylor, and L.L.Stowe, Angular Radiation models for the Earth-atmosphere system. Vol. 1 Shortwave Radiation, NASA reference Publication RP-1184, 159pp, 1989

Twomey, S. The effect of cloud scattering on the absorption of solar radiation by atmospheric dust, *J.Atmos.Sci., 29, 1156-1159, 1972*

Twomey ,S. and C.F.Bohren, Simple approximations for calculations of absorption in clouds, *J.Atmos.Sci., 37, 2086-2094, 1980*

Twohy C.H., A.D.Clarke, S.G. Warren, L.F.Radke, and R.J.Charlson, Light-absorbing material extracted from cloud droplets and its effect on cloud albedo, *J.Geophys. Res*, **94**, 8623-8631, 1989

Wellemeyer, C.G., S.L.Taylor,G.Jaross, M.T.DeLand, C.J.Seftor, G.Labow, T.J. Swissler, and R.P.Cebula, Final Report on Nimbus-7 TOMS Version 7 Calibration, NASA Contractor Report 4717, pp. 48, 1996.

Wellemeyer C. G., S.L.Taylor, C.J.Seftor, r.D. McPeters, and P.K. Bhartia, A correction for total ozone mapping spectrometer profile shape errors at high latitude, *Journ. Geophys. Res.*, **102**, 9029-9038, 1997

Wiscombe W.J., and S.G. Warren, A model for the spectral albedo of snow, I.Pure snow, *J.Atmos.Sci.*,**37**,2712-2733, 1980

Zege E.P., and A.A. Kokhanovskii, Approximate Formula for the Albedo of snow surface, *Izvestiya. Atmospheric and oceanic Physics,* **33**, 667-668, 1997